

Received August 29, 2020, accepted October 4, 2020, date of publication October 12, 2020, date of current version October 29, 2020.

Digital Object Identifier 10.1109/ACCESS.2020.3030232

An Online One-Step Method to Identify Inertial Parameters of the Base and the Target Simultaneously for Space Robots in Postcapture

TENG ZHANG¹, XIAOKUI YUE, (Member, IEEE), AND JIANPING YUAN²

School of Astronautics, Northwestern Polytechnical University (NWPU), Xi'an 710072, China
National Key Laboratory of Aerospace Flight Dynamics (AFDL), Northwestern Polytechnical University (NWPU), Xi'an 710072, China

Corresponding authors: Teng Zhang (zt_raymond@hotmail.com) and Xiaokui Yue (xkyue@nwpu.edu.cn)

This work was supported in part by the National Natural Science Foundation of China under Grant 11972026.

ABSTRACT Space robots are in free-flying or free-floating mode, motions especially attitude motion of the base and motion of the manipulator are strongly coupled. Regarding to the uncertainties of the target's inertial parameters and variation of the base's inertial parameters, this paper presents a novel online one-step parameter identification method to estimate all the inertial parameters of the target and the base simultaneously. Momentum- and force-based identification equations are derived from the linear and angular momentum equations of the system and their derivation, and the modified recursive least square method is used for solving the equations efficiently. Compared with the traditional methods, the momentum-based equation can estimate all the inertial parameters of the base and the target simultaneously at each steps, while the force-based equation does not require torque of the joints. To verify the validity and feasibility of the proposed methods, 2D and 3D models with different targets and initial velocities are simulated and analyzed. The results show that all the estimated values show convergence to their ideal values and the method can be easily achieved online via recursive techniques.

INDEX TERMS Space robot, parameter identification, target and base, online one-step.

I. INTRODUCTION

According to the Orbital Debris Quarterly News from The National Aeronautics and Space Administration (NASA), number of space debris is constantly increasing [1], and fragmentation or collision of them would enlarge their population, even if all space launches are stopped immediately [2]. Every year, it is necessary to remove at least five at 1 to 8 ton range debris to keep the population of the debris stable for further space missions [3]. Researchers have devoted a lot to space debris removal missions, details and comparison of different removal methods are showed [4]. At April 2nd, 2018, the RemoveDebris Platform was launched into International Space Station (ISS); technologies including being deployed from ISS, snaring space debris by net, reconnaissance and navigation test have been demonstrated, details can be found [5].

The associate editor coordinating the review of this manuscript and approving it for publication was Kan Liu³.

The space robot, robotic manipulator (arm) mounted on the servicing satellite (base), is regarded as one of the most promising methods for space debris removal missions [6]. Space robots including the ETS-VII and the Orbit Express have been launched successfully [7], [8]. For a space robot, the base is free-floating or free-flying, motion of the manipulator and the base is strongly coupled, estimating the inertial parameters of the captured unknown target is beneficial for path planning, as well as the control system [9].

Generally, there are two kinds of estimation methods for space robots, the momentum- and the force-based methods. Momentum-based method, which is based on the momentum theorem, only requires position, velocity of the base and angle, angular velocity of the joints. It was first conducted by Murotsu [10], with the assumption that the initial linear and angular momentum of the whole system including the base and the target are zero after capture. Thai *et al.* presented the method for estimating the inertial parameters of the unknown target in postcapture, initial linear momentum of

TABLE 1. Comparison of the different methods.

| Method | Force-based | Momentum-based |
|--------------|-------------------------------------|-----------------------|
| Based on | Newton-Euler equation | Momentum theorem |
| Measurements | Position, velocity and acceleration | Position and velocity |
| Number | Multiple bodies | Only one |
| Precision | Lower | Higher |

Measurements: Required parameters describing the motions of the base and joints of the arms

Number: Number of the bodies of which inertial parameters can be identified

Precision: Precision of the measurements

the whole system is zero while angular momentum is not [11]. Zhang *et al.* conducted an identification technique for a space robot with unknown target, initial angular or linear momentum of the system is not zero [12], [13]. Ma *et al.* used motion of the robotic arm to estimate the inertial parameters of the base [14], [15]. With the combination of momentum theorem and integration of the contact force, a two-step identification equation was derived by Chu to avoid the accumulated errors of measurements, and recursive least square (RLS)-affine projection sign algorithm was used for the equation [9]. Feng *et al.* only used the conservation of angular momentum to derive the identification equation, and the probability distribution evolution algorithm was used to identify the inertial parameters of the target [16]. Generally, the momentum-based method can only estimate inertial parameters of one-body (the base or the target) at each steps.

Compared with the momentum-based method, the force-based method utilizes dynamics of the system. Same as the momentum-based method, the force-based method was also first conducted by Murotsu [10]. Besides space robots, the force-based method can also be applied for ground robots and the identification technique can estimate inertial parameter of more than one body at each steps. For example, with the help of matrix set, Chashmi *et al.* derived the identification equation for estimating inertial parameters of all the bodies, including the base and all the links of the arm, the equation was written in the linear regression form which can be easily solved by standard methods including RLS method [17]. Ayusawa *et al.* conducted the estimation equation for the base's parameters (the minimal set of inertial parameters that describes the dynamics of the system) of the legged systems [18]. Xu *et al.* utilized the combination of the force- and the momentum-based methods to estimate inertial parameters of all the bodies step by step [19], [20]. The whole system was regarded as one-body first, as all the joints were considered locked; then the thrusters begun to work for maneuvering, and the estimation equation for the one-body was derived from the Newton-Euler equation, which belongs to the force-based method. At every sub sequential step only one joint was driven to move along the desired trajectory under the free-floating mode, and the momentum-based identification equation was used to estimate the inertial parameters of the selected body step by step. The force-based method requires torque of the joints, which is difficult to be measured accurately considering dead-zone or friction of the

joints. Comparison of the momentum- and the force-based methods is showed in Table.1.

Measurements of the momentum-based methods generally show higher accuracy, because acceleration of the base and angular acceleration of the joints are often obtained by numerical difference of velocity or angular velocity, which are more sensitive to noise, but the momentum-based method can only identify inertial parameters of a single body (the base or the target). Inertial parameters of all the bodies can be estimated, but only inertial parameters of the selected one can be estimated at each steps [19], [20]. Dynamics of multibody systems can be written in a linear form with respect to the inertial parameters [21], besides motion of the system, if force and torque of the bodies and torque of the joints can be measured, inertial parameters of all the bodies can be identified. However, estimated results of the linear form from the equation do not show convergence to their ideal values in some situations [22], [23]. So, researchers transformed the identification problem into optimization problem, which can be solved by optimization method. Vyasrayani *et al.* solved the identification equation by homotopy optimization method, the method was useful for estimating nonlinear parameters with partial measurements [24]. For the method presented by Sousa, physical feasibility of the estimated inertial parameters was written as the framework of linear matrix inequality, the estimation equation can be solved with semidefinite programming techniques [25]. Lauß adapted the discrete adjoint method for discretization of Hilber-Hughes-Taylor-solver to obtain the optimal solution of the identification equation [26]. Particle swarm optimization method was used to solve the identification equation by Xu [19], [20]. The optimization method plays significant roles in practice, but they are of high computational complexity.

For space robots, because of fuel consumption, payload deployment and such, inertial parameters of the base would change [14], [15]; therefore they cannot be obtained accurately from the ground experiments. It is essential to estimate the inertial parameters of the base as well as the captured unknown target to improve the performance. This paper presents an online one-step momentum-based method for identifying the base's and the target's inertial parameters simultaneously. Based on it, the force-based method, which does not require torque of the joints of the arms, is also conducted. Regarding to the difficulty in measuring torque of the joints, the presented method surpasses the traditional ones.

Through out the entire process, the identification equation is written in the linear form with respect to the inertial parameters being identified, and the modified RLS method conducted by Zhang [13] is used to estimate all the inertial parameters simultaneously at every step. This paper focuses on the inertial parameter identification of the base with the target after capture, the contact and orbital dynamics are not considered here.

After introduction to the background, kinematics and dynamics of a space robot will be introduced for further analyzing, and the momentum-based method for estimating the inertial parameters of the base and the target will be derived in Section III, followed by the force-based method. Next, the modified RLS method is introduced basically. The 2D and the 3D models with different initial velocities are simulated to verify the identification technique.

II. MODELING OF SPACE ROBOTS

To present the momentum- and force-based identification equations, the basic information about recursive kinematic and dynamics of a space robot is introduced first.

A. REGULAR LABELLING

Regular labelling [27] is introduced here to conduct recursive kinematics and dynamics in the next part. The number of bodies and joints are regularly labelled, or precisely, body j is connected to its inboard body i by joint j and $i < j$ as showed in Fig. 1. Suppose there are n bodies for the whole system, the base is labelled as 1 and the target is labelled as n .

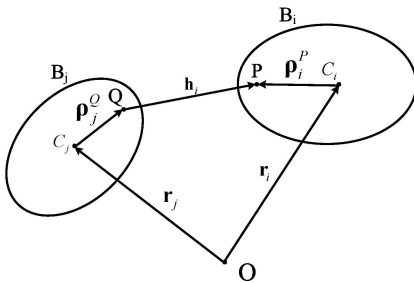


FIGURE 1. Diagram of two adjacent bodies.

It is defined that:

\mathbf{A}_j and \mathbf{A}_i : the directional cosine matrices of j -th and i -th body;

$\boldsymbol{\omega}_j$ and $\boldsymbol{\omega}_i$: the absolute angular velocity of j -th and i -th body;

$\boldsymbol{\beta}_j$ and $\boldsymbol{\beta}_i$: the absolute angular acceleration of j -th and i -th body;

\mathbf{r}_j and \mathbf{r}_i : the position vectors of the mass center of j -th and i -th body;

\mathbf{v}_j and \mathbf{v}_i : the velocity of j -th and i -th body;

\mathbf{a}_j and \mathbf{a}_i : the acceleration of j -th and i -th body;

C_j and C_i : the mass centers of j -th and i -th body;

Q and P : the joint definition points on body j and i ;

\mathbf{h}_j : the relative motion of the joint j .

Generally, the parameter is described in the inertial frame, and the superscript ' $'$ ' means that it is in the corresponding body frame.

B. KINEMATICS AND DYNAMICS

As illustrated in Fig. 1, relationship between the kinematical and the dynamical parameters of the i -th and j -th body can be written as:

$$\mathbf{r}_i = \mathbf{r}_j + \mathbf{h}_i + \boldsymbol{\rho}_j^Q + \boldsymbol{\rho}_i^P \quad (1)$$

$$\mathbf{v}_i = \mathbf{v}_j + \dot{\mathbf{h}}_i + \boldsymbol{\omega}_j \times \mathbf{h}_i + \boldsymbol{\omega}_j \times \boldsymbol{\rho}_j^Q + \boldsymbol{\omega}_i \times \boldsymbol{\rho}_i^P \quad (2)$$

$$\begin{aligned} \mathbf{a}_i = & \mathbf{a}_j + \ddot{\mathbf{h}}_i + \boldsymbol{\beta}_j \times \mathbf{h}_i + 2\boldsymbol{\omega}_j \times \dot{\mathbf{h}}_i \\ & + \boldsymbol{\beta}_j \times \boldsymbol{\rho}_j^Q + \boldsymbol{\omega}_j \times \boldsymbol{\omega}_j \times \boldsymbol{\rho}_j^Q + \boldsymbol{\beta}_i \times \boldsymbol{\rho}_i^P \\ & + \boldsymbol{\omega}_j \times \boldsymbol{\omega}_j \times \mathbf{h}_i + \boldsymbol{\omega}_i \times \boldsymbol{\omega}_i \times \boldsymbol{\rho}_i^P \end{aligned} \quad (3)$$

$$\mathbf{A}_i = \mathbf{A}_j \mathbf{A}_i^j \quad (4)$$

$$\boldsymbol{\omega}_i = \boldsymbol{\omega}_j + \boldsymbol{\omega}_j^i \quad (5)$$

$$\boldsymbol{\beta}_i = \boldsymbol{\beta}_j + \boldsymbol{\beta}_j^i \quad (6)$$

Angular momentum $\mathbf{P}(t)$ and linear momentum $\mathbf{L}(t)$ of the whole system can be written as:

$$\mathbf{P}(t) = \sum_{i=1}^n m_i \mathbf{v}_{i,t} \quad (7)$$

$$\mathbf{L}(t) = \sum_{i=1}^n \mathbf{I}_{i,t} \boldsymbol{\omega}_{i,t} + m_i \mathbf{r}_{i,t} \times \mathbf{v}_{i,t} \quad (8)$$

where m_i and \mathbf{I}_i are mass and inertia tensor of i -th body, and t refers to time.

III. IDENTIFICATION EQUATION

Here, it is assumed that only the inertial parameters of the base and the target are going to be identified. For the arm, all the inertial and geometrical parameters are known, while for the base, position of the sensor is regarded as the assumed mass center.

A. MOMENTUM-BASED METHOD

When external force and torque are applied, the corresponding linear and angular momentum can be written as:

$$\mathbf{P}(t) - \mathbf{P}(t_0) = \int_{t_0}^t \sum_{i=1}^{i=n} \mathbf{F}_i(\tau) d\tau \quad (9)$$

$$\begin{aligned} \mathbf{L}(t) - \mathbf{L}(t_0) = & \int_{t_0}^t \sum_{i=1}^{i=n} \mathbf{M}_i(\tau) d\tau \\ & + \int_{t_0}^t \sum_{i=1}^{i=n} \mathbf{r}_i(\tau) \times \mathbf{F}_i(\tau) d\tau \end{aligned} \quad (10)$$

where \mathbf{F}_i and \mathbf{M}_i refer to the external force and torque of the i -th body.

1) IDENTIFICATION OF MASS AND MASS CENTER

Combine Eqs.(7) with (9) together, after variable separation with mass and mass centers of the base and the target,

the identification equation for them can be written as:

$$[\mathbf{B}(t) - \mathbf{B}(t_0)] \begin{bmatrix} m_1 \\ m_1 \mathbf{b}'_1 \\ m_n \\ m_n \mathbf{b}'_n \end{bmatrix} = \mathbf{C}(t) - \mathbf{C}(t_0) \quad (11)$$

where m_1 and m_n are the mass of the base and the target, \mathbf{b}'_1 is the position vector from the sensor (assumed mass center) to mass center of the base in the body frame of the base, \mathbf{b}'_n is the position vector from the end-effector to mass center of the target in the body frame of the target. Details of the functions in Eq.(11) are as follows:

$$\mathbf{B}(t) = [\mathbf{v}_{1,t} \quad \tilde{\boldsymbol{\omega}}_{1,t} \mathbf{A}_{1,t} \quad \mathbf{v}_{n,t} \quad \tilde{\boldsymbol{\omega}}_{n,t} \mathbf{A}_{n,t}] \quad (12)$$

$$\mathbf{C}(t) = \int_{t_0}^t \mathbf{F}_{sum}(\tau) d\tau - \sum_{i=2}^{n-1} m_i(t) \mathbf{v}_i(t) \quad (13)$$

$\tilde{\mathbf{v}}$ indicates the following cross matrix for a vector $\mathbf{v} = [v_1, v_2, v_3]^T$.

$$\tilde{\mathbf{v}} = \begin{bmatrix} 0 & -v_3 & v_2 \\ v_3 & 0 & -v_1 \\ -v_2 & v_1 & 0 \end{bmatrix} \quad (14)$$

2) IDENTIFICATION OF INERTIA TENSOR

Suppose only the base is equipped with gas jet thrusters, and position of the thrusters relative to the sensors in the body frame of the base \mathbf{r}'_{jet} is known, then the control force term in the right side of Eq.(10) can be written as:

$$\begin{aligned} \int_{t_0}^t \sum_{i=1}^{i=n} \mathbf{r}_i(\tau) \times \mathbf{F}_i(\tau) d\tau &= \int_{t_0}^t \mathbf{r}_1(\tau) \times \mathbf{F}_1(\tau) d\tau \\ &= \int_{t_0}^t [\mathbf{r}_b(\tau) + \mathbf{A}_1(\tau) \mathbf{r}'_{jet}] \times \mathbf{F}_1(\tau) d\tau \end{aligned} \quad (15)$$

Via Eqs.(8) and (10), after variable separation, the identification equation for inertial tensor of the base and the target can be written as:

$$\begin{aligned} [\mathbf{D}(t) - \mathbf{D}(t_0)] \begin{bmatrix} \mathbf{I}'_1 \# \\ \mathbf{I}'_n \# \end{bmatrix} &= \mathbf{E}(t) - \mathbf{E}(t_0) \\ &\quad - \mathbf{H}_1(t) m_1 \mathbf{J}(\mathbf{b}'_1) \\ &\quad - \mathbf{H}_n(t) m_n \mathbf{J}(\mathbf{b}'_n) \end{aligned} \quad (16)$$

where

$$\mathbf{D}(t) = [\mathbf{A}_{1,t} [\#(\mathbf{A}_{1,t}^T \boldsymbol{\omega}_{1,t})] \quad \mathbf{A}_{n,t} [\#(\mathbf{A}_{n,t}^T \boldsymbol{\omega}_{n,t})]] \quad (17)$$

$$\begin{aligned} \mathbf{E}(t) &= \int_{t_0}^t \{ \mathbf{M}_{sum}(\tau) + [\mathbf{r}_b(\tau) + \mathbf{A}_1(\tau) \mathbf{r}'_{jet}] \\ &\quad \times \mathbf{F}_1(\tau) \} d\tau \\ &\quad - \sum_{i=2}^{i=n-1} [m_i \mathbf{r}_i(\tau) \times \mathbf{v}_i(t) + \mathbf{I}_i(t) \boldsymbol{\omega}_i(t)] \end{aligned} \quad (18)$$

$$m_i \mathbf{r}_{i,t} \times \mathbf{v}_{i,t} = \mathbf{H}_i(t) m_i \mathbf{J}(\mathbf{b}'_i) \quad (i = 1 \text{ or } n) \quad (19)$$

$[\#\bullet]$ indicates the following operation matrix for a vector $\mathbf{v} = [v_1, v_2, v_3]^T$.

$$[\#\mathbf{v}] = \begin{bmatrix} v_1 & v_2 & v_3 & 0 & 0 & 0 \\ 0 & v_1 & 0 & v_2 & v_3 & 0 \\ 0 & 0 & v_1 & 0 & v_2 & v_3 \end{bmatrix} \quad (20)$$

The vector $[\bullet\#]$ indicates the following operation vector

$$[\mathbf{I}\#] = [I_{11} \quad I_{12} \quad I_{13} \quad I_{22} \quad I_{23} \quad I_{33}] \quad (21)$$

for a symmetric matrix

$$\mathbf{I} = \begin{bmatrix} I_{11} & I_{12} & I_{13} \\ I_{12} & I_{22} & I_{23} \\ I_{13} & I_{23} & I_{33} \end{bmatrix} \quad (22)$$

$$\mathbf{J}(\mathbf{b}'_i) = [1 \ b'_x \ b'_y \ b'_z \ b'_x{}^2 \ b'_x b'_y \ b'_x b'_z \ b'_y{}^2 \ b'_y b'_z \ b'_z{}^2]^T \quad (23)$$

Details of the matrices $\mathbf{H}_1(t)$ and $\mathbf{H}_n(t)$ are showed in APPENDIX A.

B. FORCE-BASED METHOD

According to [28], derivation of the directional cosine matrix with respect to time is:

$$\frac{d\mathbf{A}}{dt} = \tilde{\boldsymbol{\omega}} \mathbf{A} \quad (24)$$

So, it is easily written that:

$$\frac{d(\mathbf{I}\boldsymbol{\omega})}{dt} = \frac{d(\mathbf{A}\mathbf{I}'\mathbf{A}'\boldsymbol{\omega})}{dt} = \mathbf{I}\boldsymbol{\beta} + \tilde{\boldsymbol{\omega}}\mathbf{I}\boldsymbol{\omega} + \mathbf{I}\tilde{\boldsymbol{\omega}}\boldsymbol{\omega} \quad (25)$$

Derivate Eqs.(7) and (9) with respect to time together:

$$\sum_{i=1}^{i=n} \mathbf{F}_{i,t} = \sum_{i=1}^{i=n} m_i \mathbf{a}_{i,t} \quad (26)$$

With the help of Eqs.(24) and (25), derivate Eq. (10) with respect to time, it can be obtained that:

$$\begin{aligned} \sum_{i=1}^n \mathbf{M}_{i,t} + \sum_{i=1}^n \mathbf{r}_{i,t} \times \mathbf{F}_{i,t} &= \sum_{i=1}^n \mathbf{I}_{i,t} \boldsymbol{\beta}_{i,t} \\ &\quad + \boldsymbol{\omega}_{i,t} \times (\mathbf{I}_{i,t} \boldsymbol{\omega}_{i,t}) + m_i \mathbf{r}_{i,t} \times \mathbf{a}_{i,t} \end{aligned} \quad (27)$$

As with the momentum-based method, the force-based identification equations can also be obtained after variable separation. The identification equations for mass, mass center and inertia tensor are obtained separately.

1) IDENTIFICATION OF MASS AND MASS CENTER

The identification equation for mass and mass centers of the base and the target is showed first. Via Eq.(26), after variable separation, the identification equation can be written as:

$$\mathbf{G}(t) \begin{bmatrix} m_1 \\ m_1 \mathbf{b}'_1 \\ m_n \\ m_n \mathbf{b}'_n \end{bmatrix} = \mathbf{K}(t) \quad (28)$$

where

$$\mathbf{G}(t) = [\mathbf{a}_{1,t} (\tilde{\boldsymbol{\beta}}_{1,t} + \tilde{\boldsymbol{\omega}}_{1,t} \tilde{\boldsymbol{\omega}}_{1,t}) \mathbf{A}_1 \quad \mathbf{a}_{n,t} (\tilde{\boldsymbol{\beta}}_{n,t} + \tilde{\boldsymbol{\omega}}_{n,t} \tilde{\boldsymbol{\omega}}_{n,t}) \mathbf{A}_n] \quad (29)$$

$$\mathbf{K}(t) = \sum_{i=1}^n \mathbf{F}_{i,t} - \sum_{i=2}^{n-1} m_i \mathbf{a}_i \quad (30)$$

2) IDENTIFICATION OF INERTIA TENSOR

The identification equation for inertia tensor of the base and the target is showed here, as with the momentum-based method, via Eq.(27), it can be written as:

$$\mathbf{Q}(t) \begin{bmatrix} [\mathbf{I}'_1 \#] \\ [\mathbf{I}'_n \#] \end{bmatrix} = \mathbf{R}(t) - \mathbf{S}_1(t) m_1 \mathbf{J}(\mathbf{b}'_1) - \mathbf{S}_n(t) m_n \mathbf{J}(\mathbf{b}'_n) \quad (31)$$

where

$$\begin{aligned} \mathbf{Q}(t) &= [\mathbf{Q}_1(t) \quad \mathbf{Q}_n(t)] \quad (32) \\ \mathbf{R}(t) &= \sum_{i=1}^n \mathbf{M}_{i,t} + \sum_{i=1}^n \mathbf{r}_{i,t} \times \mathbf{F}_{i,t} \\ &\quad - \sum_{i=2}^{n-1} [\mathbf{I}_{i,t} \boldsymbol{\beta}_{i,t} + \tilde{\boldsymbol{\omega}}_{i,t} \mathbf{I}_{i,t} \boldsymbol{\omega}_{i,t} \\ &\quad + \mathbf{I}_{i,t} \tilde{\boldsymbol{\omega}}_{i,t} \boldsymbol{\omega}_{i,t} + m_i \mathbf{r}_{i,t} \times \mathbf{a}_{i,t}] \quad (33) \end{aligned}$$

Details of the matrices $\mathbf{Q}_1(t)$, $\mathbf{Q}_n(t)$, $\mathbf{S}_1(t)$ and $\mathbf{S}_n(t)$ are showed in APPENDIX B and APPENDIX C. Compared with the momentum-based method Eqs.(11) and (16), for the force-based method Eqs.(28) and (31), integration is not required here. At every step of identification, for the force-based method, origin of the reference frame is the position of the sensor of the base; which varies with motion of the base, while for the momentum-based method, origin of the reference frame is origin of inertial frame because of the integration term in Eq.(18).

IV. SOLUTION METHOD

The traditional RLS method can be used in real time applications because of its low computation complexity [29], however, when it is utilized to solve the identification equations as Eqs.(11) and (16) or (28) and (31), they can only be solved by two steps. The modified RLS method has been presented by Zhang et al. [13], which can be used to solve Eqs.(11) and (16) or (28) and (31) in one-step. The method is utilized here to obtain the inertial parameters of the base and the target simultaneously, it is briefly introduced here. For the identification equations presented in this paper Eqs.(11) and (16) or (28) and (31), the standard form can be written as:

$$\mathbf{A}\boldsymbol{\mu} = \mathbf{b} \quad (34)$$

$$\boldsymbol{\phi}\boldsymbol{\theta} = \mathbf{y} + \boldsymbol{\psi}\mathbf{D}(\boldsymbol{\mu}) \quad (35)$$

where the regressor matrices \mathbf{A} , $\boldsymbol{\phi}$, the output vectors \mathbf{b} , \mathbf{y} and the matrix $\boldsymbol{\psi}$ vary with time. Here, $\boldsymbol{\mu}$ represents m_1 , \mathbf{b}'_1 , m_n and \mathbf{b}'_n , while $\boldsymbol{\theta}$ represents the estimated values of inertia tensor $[\mathbf{I}'_1 \#]$ and $[\mathbf{I}'_n \#]$. The term $\boldsymbol{\psi}\mathbf{D}(\boldsymbol{\mu})$ is from the second-order term $m_1 \mathbf{r}_1 \times \mathbf{v}_1$ and $m_n \mathbf{r}_n \times \mathbf{v}_n$ in Eq.(8) for the momentum-based method, and their derivatives in Eq.(27) for the force-based one.

For the traditional RLS method, estimated values of $\boldsymbol{\mu}$ are obtained first by solving Eq.(34), then the RLS method is applied again to estimate values of $\boldsymbol{\theta}$. However, estimating all the inertial parameters by two-step method is not beneficial for online identification because it would cost more time for the space robot to move or more storage to save the data. Suppose there are N sets of data, and the results obtained

TABLE 2. Parameters of the 2D model.

| Body | Mass(kg) | I(kgm ²) |
|---------------|----------|----------------------|
| Base | 500 | 83.61 |
| Link1 | 10 | 1.05 |
| Link2 | 10 | 1.05 |
| Link3 | 10 | 1.05 |
| Small target | 125 | 5.2 |
| Medium target | 250 | 10.41 |
| Large target | 500 | 20.83 |

by the traditional two-step identification technique are $\boldsymbol{\mu}_N$ and $\boldsymbol{\theta}_N$ separately. If a new set of data is applied, the corresponding estimated results are $\boldsymbol{\mu}_{N+1}$ and $\boldsymbol{\theta}_{N+1}$. It is obvious that $\boldsymbol{\mu}_{N+1}$ can be obtained easily with one-step iteration by the traditional RLS method. However, for obtaining $\boldsymbol{\theta}_{N+1}$, iteration needs to be done from beginning again according to the original two-step method. To avoid it, the modified RLS method is showed here and $\boldsymbol{\theta}_{a,b}$ is introduced, the subscript a means that the result is obtained after a -step iteration, while b means that the estimated result corresponds to $\boldsymbol{\mu}_b$.

According to the traditional RLS method [13], [29], for Eq.(35), it can be easily written that:

$$\boldsymbol{\theta}_{N,N+1} - \boldsymbol{\theta}_{N,N} = \mathbf{M}(N) [\mathbf{D}(\boldsymbol{\mu}_{N+1}) - \mathbf{D}(\boldsymbol{\mu}_N)] \quad (36)$$

and

$$\begin{aligned} \boldsymbol{\theta}_{N-1,N} - \boldsymbol{\theta}_{N-1,N-1} \\ = \mathbf{M}(N-1) [\mathbf{D}(\boldsymbol{\mu}_N) - \mathbf{D}(\boldsymbol{\mu}_{N-1})] \quad (37) \end{aligned}$$

where

$$\mathbf{M}(N) = (\mathbf{I} - \mathbf{K}_N \boldsymbol{\phi}_N^T) \mathbf{M}(N-1) + \mathbf{K}_N \boldsymbol{\psi}_N \quad (38)$$

and $\mathbf{M}(0) = \mathbf{0}$.

V. SIMULATION

To verify the identification technique, numerical simulations of different scenarios are carried out in this section. In all the scenarios, it is assumed that the end-effector grasps the target firmly. The 2D and the 3D models are illustrated in Figs. 2 and 3, and parameters of the 2D and the 3D models are showed in Tables. 2 and 3.

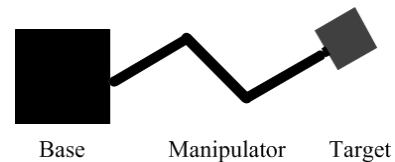


FIGURE 2. 2D simulation model.

The recursive dynamics presented by Wittenburg [27] is used and simulations are run on the C platform. The fourth-order Runge-Kutta numerical integration method is used with the time step of 10^{-3} s, while the sampling period for the measurements is 0.1 s. The control scheme [12], which utilizes the motion of the manipulator to stabilize the base's

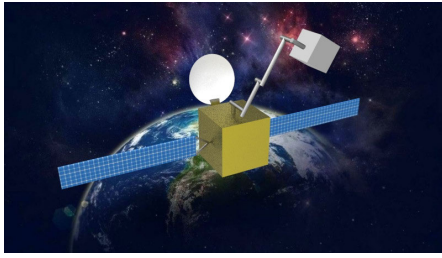


FIGURE 3. 3D simulation model.

TABLE 3. Parameters of the 3D model.

| Category | Mass [kg] | I_{xx} [kgm ²] | I_{yy} [kgm ²] | I_{zz} [kgm ²] |
|----------|-----------|------------------------------|------------------------------|------------------------------|
| Base | 500 | 83.33 | 83.33 | 83.33 |
| Link 1 | 22.7 | 3.14×10^{-2} | 3.13×10^{-2} | 5.70×10^{-2} |
| Link 2 | 45.3 | 0.99 | 5.10×10^{-2} | 1.03 |
| Link 3 | 61.1 | 2.67 | 5.77×10^{-2} | 2.71 |
| Link 4 | 14.0 | 5.00×10^{-2} | 4.40×10^{-3} | 4.96×10^{-2} |
| Link 5 | 14.0 | 4.40×10^{-3} | 5.00×10^{-2} | 4.96×10^{-2} |
| Link 6 | 10.1 | 2.22×10^{-2} | 3.16×10^{-3} | 2.21×10^{-2} |
| Target | 503.76 | 20.83 | 20.83 | 20.83 |

attitude rapidly is used here. Designed attitude angles of the base follow:

$$\ddot{\mathbf{q}} + \mathbf{K}_D \dot{\mathbf{q}} + \mathbf{K}_P \mathbf{q} = \mathbf{0} \quad (39)$$

when the coefficient matrices \mathbf{K}_D and \mathbf{K}_P are symmetric and positive defined, the attitude angles converge to zero (the desired attitude) finally. The bounded control torque M and force F are used to balance the angular and linear momentum of the system. Which follows:

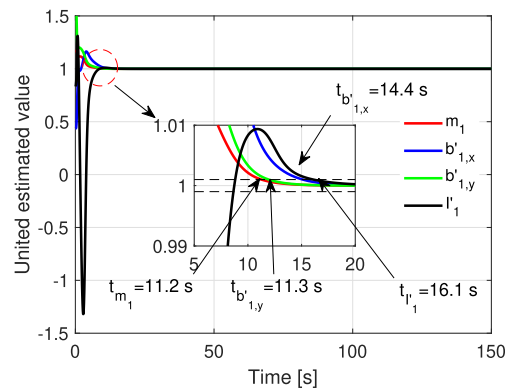
$$M = \begin{cases} -M_{max}, & \text{if } L \geq L_{max} \\ K_M \cdot L, & \text{if } L < L_{max} \text{ and } L \geq -L_{max} \\ M_{max}d, & \text{if } L \leq -L_{max} \end{cases} \quad (40)$$

$$F = \begin{cases} -F_{max}, & \text{if } P \geq P_{max} \\ K_F \cdot P, & \text{if } P < P_{max} \text{ and } P \geq -P_{max} \\ F_{max}, & \text{if } P \leq -P_{max} \end{cases} \quad (41)$$

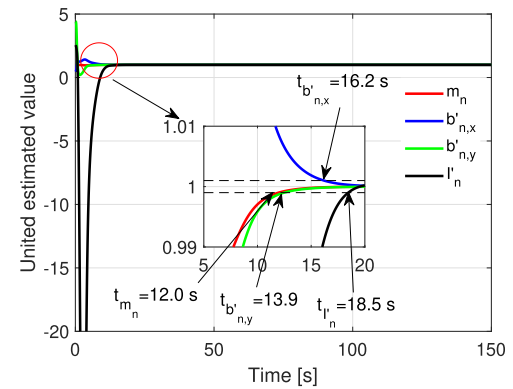
where $F_{max} = 10$ N, $K_F = -1/s$, $P_{max} = 10$ kgm/s, $M_{max} = 10$ Nm, $K_M = -1/s$ and $L_{max} = 10$ kgm²/s. For the 2D model, initial angular velocity of the base is $\omega_1 = 0.1$ rad/s while initial velocity is $\mathbf{v}_1 = [1, 2]^T$ m/s. To stabilize the base, $\mathbf{K}_D = \text{diag}(\frac{\sqrt{2}}{2})$ and $\mathbf{K}_P = \text{diag}(\frac{1}{4})$. It is supposed that the initial estimated inertial parameters of the base is $m_1 = 600$ kg, $\mathbf{b}_1 = [0, 0]^T$ m and $I_1 = 100$ kgm², while for the target $m_n = 100$ kg, $\mathbf{b}_n = [0.1, 0.1]^T$ m and $I_n = 10$ kgm² in all the scenarios. The initial identification matrix is $\mathbf{P}_{lim} = \text{diag}(10^6, 10^6, 10^6)$ for mass and mass center, and $\mathbf{P}_{ang} = \text{diag}(10^6)$ for inertia tensor. For the 3D model, initial angular velocity is $\omega = [0.1, 0.2, 0.3]^T$ rad/s and initial velocity is $\mathbf{v} = [10, 20, 30]^T$ m/s. The initial assumed inertial parameters of the base are $m_1 = 600$ kg, $\mathbf{b}'_1 = [0, 0, 0]^T$ m and $\mathbf{I}'_1 = \text{diag}(100, 100, 100)$ kgm², while for the target, they are $m_n = 100$ kg, $\mathbf{b}'_n = [0.1, 0.1, 0.1]^T$ m and $\mathbf{I}'_n = \text{diag}(10, 10, 10)$ kgm².

A. 2D MODEL

Results of the 2D model with small, medium and large targets are showed first. For the medium target, results of the estimated values with respect to time are showed while for the large and the small targets, only the final estimated values and the transit time of the estimated parameters are showed for simplification. Regarding to the influence of the integration term in the identification equation Eq.(18), situations where the 2D model with different initial velocities after capturing the medium target are simulated, and relative errors of the final estimated values with respect to the initial velocity of the base are showed.



(a) Base



(b) Target

FIGURE 4. Unitized estimated inertial parameters of the momentum-based method.

1) MEDIUM TARGET

Estimated results of the medium target are showed in Figs. 4 and 5. To compare the transit time of different estimated parameters, the estimated values are unitized by dividing their ideal values, in Figs. 4 and 5, the unitized value equals to 1 means that the corresponding parameter converges to its ideal value.

As illustrated in Figs. 4 and 5, all the estimated parameters converge to their ideal values, for the momentum-based method, the final estimated values are $m_1 = 500.00$ kg, $b'_{1,x} = 0.10$ m, $b'_{1,y} = -0.10$ m, $I'_1 = 83.61$ kgm²,

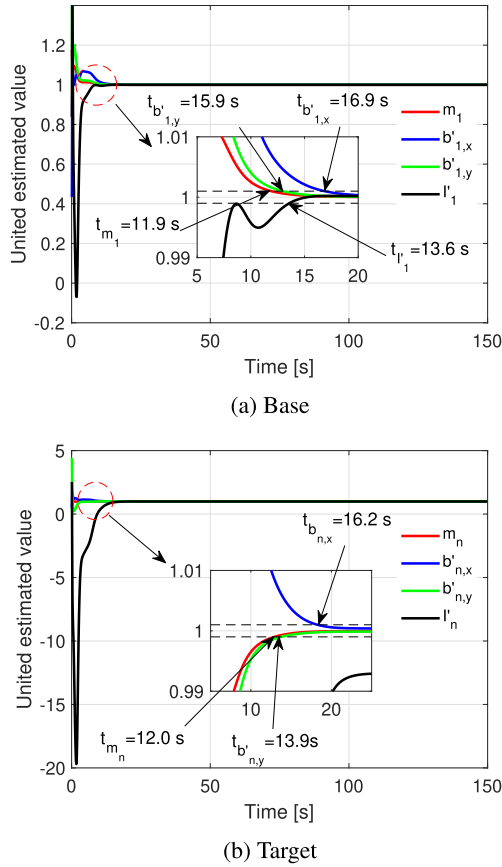


FIGURE 5. Unitized estimated inertial parameters of the force-based method.

$m_n = 250.00$ kg, $b'_{n,x} = 0.25$ m, $b_{n,y} = 0.10$ m and $I'_n = 10.41$ kgm², while for the force-base method, $m_1 = 500.01$ kg, $b'_{1,x} = 0.10$ m, $b'_{1,y} = -0.10$ m, $I'_1 = 83.62$ kgm², $m_n = 249.99$ kg, $b'_{n,x} = 0.25$ m, $b'_{n,y} = 0.10$ m and $I'_n = 10.34$ kgm². In Figs. 4 and 5, the areas between the black dotted lines mean that the relative error of the estimated value is less than 0.1%.

The time in Figs. 4 and 5 is the transit time when the relative error of the estimated result is less than 0.1%. However, in Fig. 5, the transit time for I'_n is not showed, because its final estimated value is 10.34 kgm², the corresponding relative error is 0.67%, which is larger than 0.1%. It can be seen that the transit time of inertia tensor especially I'_n is longer both in the momentum- and force-based methods. This is because that results of the estimated mass and mass center have influence on the estimated values of inertia tensor as in the identification equation of inertia tensor Eqs. (16) and (28).

The momentum-based method provides better estimation results especially I'_n , because norm of the change of velocity $\|\mathbf{v}(t) - \mathbf{v}(0)\|$ is larger than the norm of acceleration, so the elements of the regressor matrix in the identification equation Eq.(16) are larger with the same accuracy of the data, it has better results. Better estimated m_n and \mathbf{b}'_n result in better identified I'_n . In the momentum- and force-based methods,

the transit time for the inertial parameters of the base is shorter than that of the target, because the initial values of the base's identified parameters are closer to the ideal ones.

2) SMALL AND LARGE TARGET

Identification results of the small and the large targets from the momentum- and force-based methods are showed in Table. 4 and 5, values in the brackets are the transit time. The transit time of I'_n for the force-based method is not showed, because the relative error of the final estimated value is 0.6%, which is larger than 0.1%. As with the estimated results of the medium target, the momentum-based method provides better estimation, especially for I'_n , and often it costs more time for inertia tensor to converge to the ideal value especially I'_n . For the 2D model, in simulation the initial inertial parameters of the base and the target are supposed to be same, which are closer to the ideal values of the small target, so the transit time of the small target is the shorter in generally.

TABLE 4. Estimated values of the small target.

| Category | Ideal values | Estimated values | |
|----------------------------|--------------|-----------------------|--------------------|
| | | Momentum-based method | Force-based method |
| m_1 [kg] | 500 | 500.00 (9.5 s) | 500.00 (9.2 s) |
| $b'_{1,x}$ [m] | 0.10 | 0.10 (10.9 s) | 0.10 (11.0 s) |
| $b'_{1,y}$ [m] | -0.1 | -0.10 (9.4 s) | -0.10 (9.4 s) |
| I'_1 [kgm ²] | 83.61 | 83.61 (12.5 s) | 83.62 (11.8 s) |
| m_n [kg] | 125 | 125.00 (10.6 s) | 125.00 (10.6 s) |
| $b'_{n,x}$ [m] | 0.25 | 0.25 (13.2 s) | 0.25 (14.0 s) |
| $b'_{n,y}$ [m] | 0.10 | 0.10 (9.6 s) | 0.10 (9.2 s) |
| I'_n [kgm ²] | 5.20 | 5.20 (13.4 s) | 5.19 (18.7 s) |

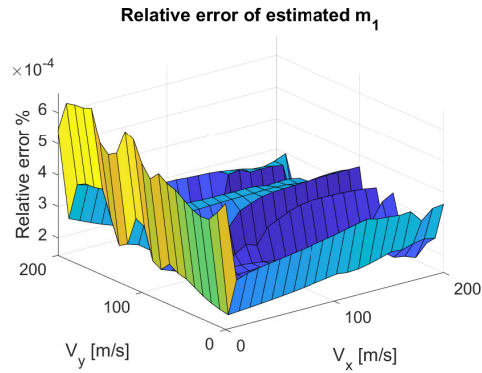
TABLE 5. Estimated values of the large target.

| Category | Ideal values | Estimated values | |
|----------------------------|--------------|-----------------------|--------------------|
| | | Momentum-based method | Force-based method |
| m_1 [kg] | 500 | 500.00 (13.3 s) | 500.02 (15.0 s) |
| $b'_{1,x}$ [m] | 0.10 | 0.10 (17.4 s) | 0.10 (21.7 s) |
| $b'_{1,y}$ [m] | -0.1 | -0.10 (18.7 s) | -0.10 (17.2 s) |
| I'_1 [kgm ²] | 83.61 | 83.61 (19.2 s) | 83.62 (20.5 s) |
| m_n [kg] | 500 | 500.00 (12.1 s) | 499.98 (13.6 s) |
| $b'_{n,x}$ [m] | 0.25 | 0.25 (17.2 s) | 0.25 (20.7 s) |
| $b'_{n,y}$ [m] | 0.10 | 0.10 (14 s) | 0.10 (17.1 s) |
| I'_n [kgm ²] | 20.83 | 20.83 (20.9 s) | 20.70 (-) |

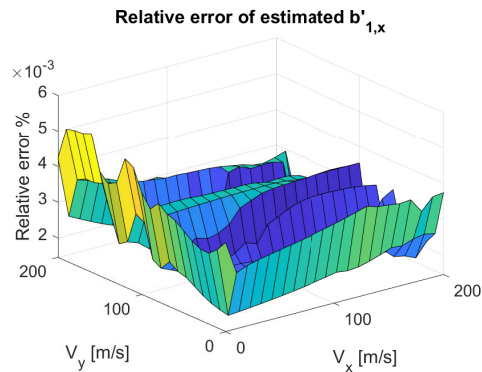
3) ANALYSE

In Eq.(18), we can see that the estimated mass, mass center, and position of the base and the target all have influence on the identification of inertia tensor of the base and the target. Situations for the medium target with different initial velocities are simulated. To show the influence more obviously, the maximal magnitude of the control force is much smaller, 0.1 N. In Figs. 4 and 5, the time consumption that the estimated values converge to the ideal values is less than 20 s, so the estimated results at 60 s are analyzed. Figs. 6-9 show the relative error of the estimated values with the different velocity of the base.

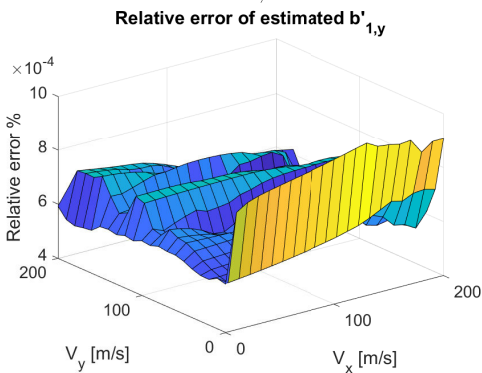
In Figs. 6-9, for the two methods, error of the estimated mass and mass center does not vary dramatically with the



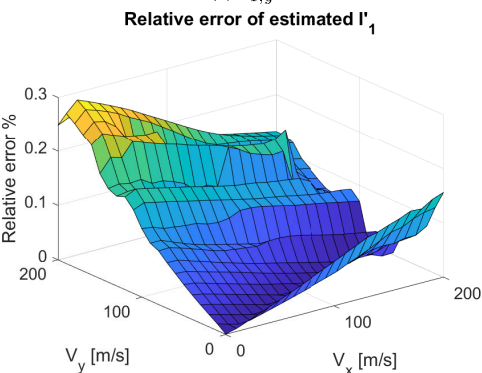
(a) m_1



(b) $b'_{1,x}$

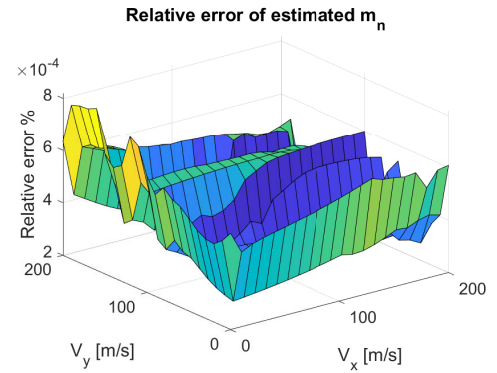


(c) $b'_{1,y}$

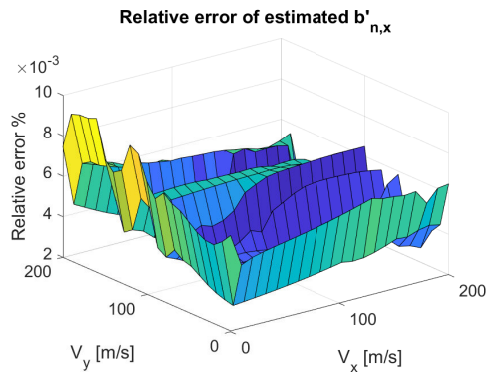


(d) I'_1

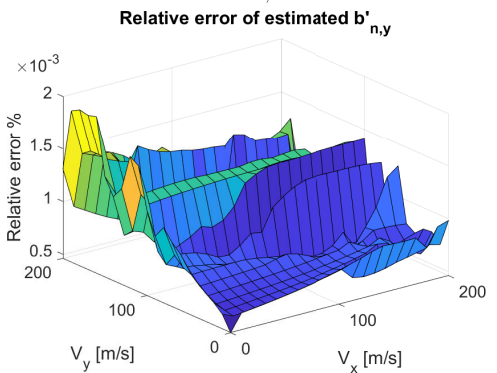
FIGURE 6. Relative error of the estimated inertial parameters of the base for the momentum-based method with different initial velocity.



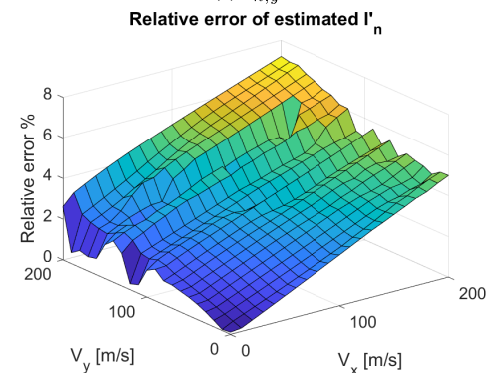
(a) m_n



(b) $b'_{n,x}$



(c) $b'_{n,y}$



(d) I'_n

FIGURE 7. Relative error of the estimated inertial parameters of the target for the momentum-based method with different initial velocity.

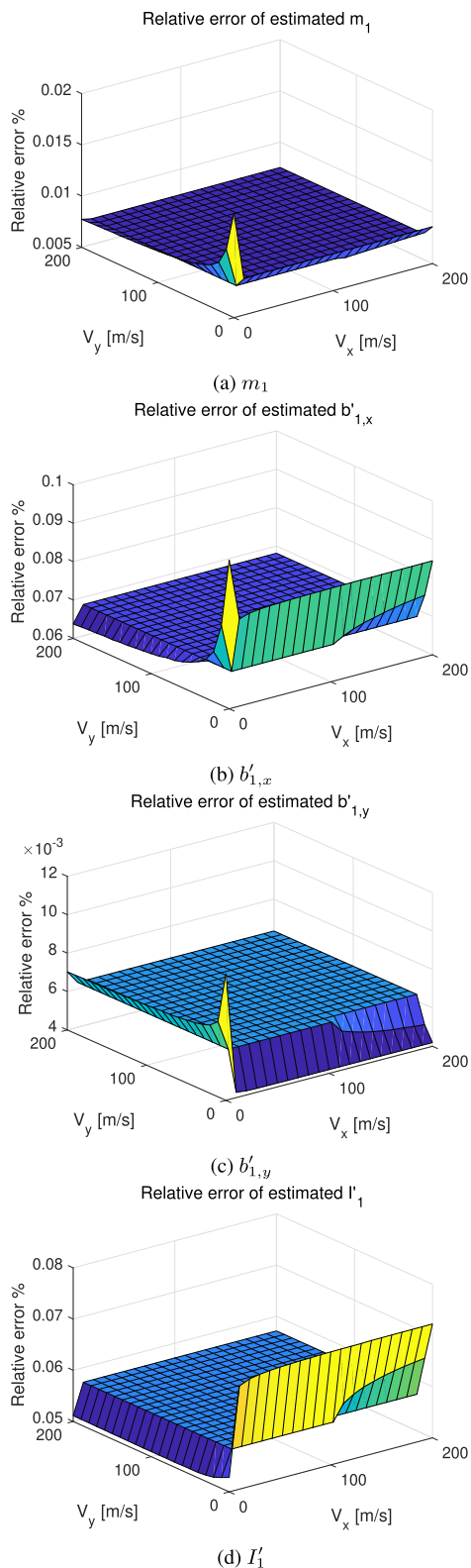


FIGURE 8. Relative error of the estimated inertial parameters of the base for the force-based method with different initial velocity.

initial velocity, while the estimated inertia tensor shows different results. For the momentum-based method, larger initial velocity of the base would make larger error of the

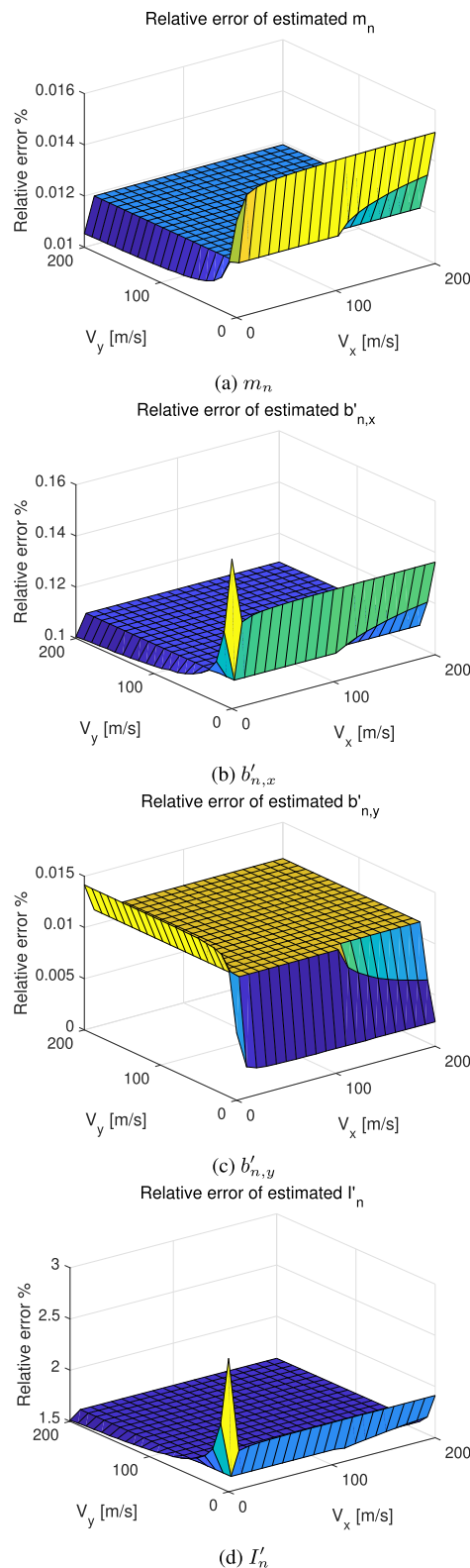


FIGURE 9. Relative error of the estimated inertial parameters of the target for the force-based method with different initial velocity.

estimated I'_n generally, the minimal relative error is about $6.6 \times 10^{-2}\%$ with the initial velocity $\mathbf{v} = [0, 10]^T$ m/s, while the maximal relative error is about 7.2% with the initial

TABLE 6. Estimated values of the 3D model.

| Category | Ideal values | Estimated values | |
|---------------------------------|--------------------------|----------------------------------|----------------------------------|
| | | Momentum-based method | Force-based method |
| m_1 [kg] | 500 | 500.00 (6.6 s) | 500.00 (0.6 s) |
| $b'_{1,x}$ [m] | 0.05 | 0.05 (1.7 s) | 0.05 (3.0 s) |
| $b'_{1,y}$ [m] | 0.05 | 0.05 (3.8 s) | 0.05 (1.9 s) |
| $b'_{1,z}$ [m] | 0.05 | 0.05 (6.3 s) | 0.05 (4.9 s) |
| $I'_{1,xx}$ [kgm ²] | 83.33 | 83.36 (84.5 s) | 83.33 (2.3 s) |
| $I'_{1,yy}$ [kgm ²] | 83.33 | 83.40 (94.20 s) | 83.33 (1.1 s) |
| $I'_{1,zz}$ [kgm ²] | 83.33 | 83.40 (95.0 s) | 83.33 (1.0 s) |
| m_n [kg] | 503.76 | 503.76(2.2 s) | 503.76 (1.8 s) |
| $b'_{n,x}$ [m] | -208.86×10^{-3} | -208.86×10^{-3} (1.6 s) | -208.86×10^{-3} (2.6 s) |
| $b'_{n,y}$ [m] | 0.49×10^{-3} | 0.490×10^{-3} (8.2 s) | 0.490×10^{-3} (14.3 s) |
| $b'_{n,z}$ [m] | 0 | 0.25×10^{-8} (27.0 s) | 0.25×10^{-11} (30.5 s) |
| $I'_{n,xx}$ [kgm ²] | 20.83 | 20.82 (33.7 s) | 20.83 (3.4 s) |
| $I'_{n,yy}$ [kgm ²] | 20.83 | 20.82 (33.5 s) | 20.83 (4.7 s) |
| $I'_{n,zz}$ [kgm ²] | 20.83 | 20.80 (-) | 20.83 (6.4 s) |

velocity $\mathbf{v} = [200, 200]^T$ m/s. However, for the force-based method, the initial velocity of the base does not show obvious influence, it can be seen that in most situations the relative errors are same. The reason is that, for the momentum-based method, in the identification equation for inertia tensor Eqs.(16)-(23), the change of angular momentum is required, so origin of the reference frame is same all the time, while for the force-based method, in every identification step, the assumed mass center of the base is selected as origin of the reference frame. For the momentum-based method, the norm of r_n increases with the increase of initial velocity, with same accuracy of the estimated mass and mass center, larger r_n would result in larger error as showed in the right hand side of the Eq.(18), then larger error of the estimated I'_n would be produced. However, for I'_1 , the estimated value is much closer to the ideal value, thus it converges to the ideal value early, the phenomenon is not so obvious, but it still can be seen that the best estimated results locate at the situation where the initial velocity is zero.

B. 3D MODEL

The identification results from the momentum- and force-based methods are showed in Table. 6. As with the results of the 2D model, the values in brackets are the transit time that relative error of the estimated value becomes less than 1%. For $b'_{n,y}$, the ideal value is 0, here the transit time means that the absolute value of the estimated $b'_{n,y}$ is less than 10^{-8} . All the estimated values showed convergence to their ideal values if enough time was given. Generally, for the force-based method; especially for the inertial parameters of the base, the transit time is significantly shorter. The reason for this is that in simulation, attitude motion of the base is not as obvious as the 2D model, so the transit time is longer.

VI. CONCLUSION

Bases of space robots are free-floating or free-flying, motions especially attitude motion of the base and motion of the manipulator are strongly coupled. Having knowledge about the inertial parameters of the whole system, including the

robot and the target, is essential for the precise control of space robots. This paper presents an identification technique for estimating all the inertial parameters of the base and the unknown target simultaneously for space robots in postcapture. The momentum-based method is derived from the angular and linear momentum equations of the space robot, while the force-based one is from their derivatives. To estimate all the inertial parameters in one step, the second-order term $m_1 \mathbf{r}_1 \times \mathbf{v}_1$ and $m_n \mathbf{r}_n \times \mathbf{v}_n$ and their derivatives are written as the product of the function of time and function of the estimated mass and mass centers in the identification equations, and the modified RLS method is utilized. Compared with the traditional momentum-based method, inertial parameters of the base and the target can be estimated simultaneously for the method in this paper. The presented force-based method surpasses the traditional ones in terms of requirement: torque of the joints is not required to be known. All the inertial parameters can be identified by the recursive method, which is beneficial for the online identification.

APPENDIX A

DETAILS OF THE MATRICES $H_1(t)$ AND $H_n(t)$

When $i = 1$ orn, it is defined that:

$$\mathbf{A}_i(t) = \begin{bmatrix} a_{i,t,1,1} & a_{i,t,1,2} & a_{i,t,1,3} \\ a_{i,t,2,1} & a_{i,t,2,2} & a_{i,t,2,3} \\ a_{i,t,3,1} & a_{i,t,3,2} & a_{i,t,3,3} \end{bmatrix} \quad (42)$$

$$\boldsymbol{\omega}_i(t) = [\omega_{i,t,x} \quad \omega_{i,t,y} \quad \omega_{i,t,z}]^T \quad (43)$$

$$\boldsymbol{\beta}_i(t) = [\beta_{i,t,x} \quad \beta_{i,t,y} \quad \beta_{i,t,z}]^T \quad (44)$$

$$\mathbf{r}_i(t) = [r_{i,t,x} \quad r_{i,t,y} \quad r_{i,t,z}]^T \quad (45)$$

$$\mathbf{v}_i(t) = [v_{i,t,x} \quad v_{i,t,y} \quad v_{i,t,z}]^T \quad (46)$$

$$\mathbf{a}_i(t) = [a_{i,t,x} \quad a_{i,t,y} \quad a_{i,t,z}]^T \quad (47)$$

\mathbf{r}_1 , \mathbf{v}_1 and \mathbf{a}_1 are the position, velocity and acceleration of the sensor, not the centerid of the base, while \mathbf{r}_n , \mathbf{v}_n and \mathbf{a}_n are the position, velocity and acceleration of capture point on the end-effector.

For $\mathbf{H}_{1,t}$ and $\mathbf{H}_{n,t}$,

$$\mathbf{H}_i(t) (t) = (h_{i,t})_{m \times l} \quad (48)$$

where

$$\begin{aligned} h_{i,t,1,1} &= r_{i,t,y}v_{i,t,z} - r_{i,t,z}v_{i,t,y} \\ h_{i,t,1,2} &= a_{i,t,2,1}v_{i,t,z} - a_{i,t,3,1}v_{i,t,y} \\ &\quad + r_{i,t,y}(a_{i,t,2,1}\omega_{i,t,x} - a_{i,t,1,1}\omega_{i,t,y}) \\ &\quad + r_{i,t,z}(a_{i,t,3,1}\omega_{i,t,x} - a_{i,t,1,1}\omega_{i,t,z}) \\ h_{i,t,1,3} &= a_{i,t,2,2}v_{i,t,z} - a_{i,t,3,2}v_{i,t,y} \\ &\quad + r_{i,t,y}(a_{i,t,2,2}\omega_{i,t,x} - a_{i,t,1,2}\omega_{i,t,y}) \\ &\quad + r_{i,t,z}(a_{i,t,3,2}\omega_{i,t,x} - a_{i,t,1,2}\omega_{i,t,z}) \\ h_{i,t,1,4} &= a_{i,t,2,3}v_{i,t,z} - a_{i,t,3,3}v_{i,t,y} \\ &\quad + r_{i,t,y}(a_{i,t,2,3}\omega_{i,t,x} - a_{i,t,1,3}\omega_{i,t,y}) \\ &\quad + r_{i,t,z}(a_{i,t,3,3}\omega_{i,t,x} - a_{i,t,1,3}\omega_{i,t,z}) \\ h_{i,t,1,5} &= a_{i,t,2,1}(a_{i,t,2,1}\omega_{i,t,x} - a_{i,t,1,1}\omega_{i,t,y}) \\ &\quad + a_{i,t,3,1}(a_{i,t,3,1}\omega_{i,t,x} - a_{i,t,1,1}\omega_{i,t,z}) \\ h_{i,t,1,6} &= a_{i,t,2,2}(a_{i,t,2,1}\omega_{i,t,x} - a_{i,t,1,1}\omega_{i,t,y}) \\ &\quad + a_{i,t,2,1}(a_{i,t,2,2}\omega_{i,t,x} - a_{i,t,1,2}\omega_{i,t,y}) \\ &\quad + a_{i,t,3,2}(a_{i,t,3,1}\omega_{i,t,x} - a_{i,t,1,1}\omega_{i,t,z}) \\ &\quad + a_{i,t,3,1}(a_{i,t,3,2}\omega_{i,t,x} - a_{i,t,1,2}\omega_{i,t,z}) \\ h_{i,t,1,7} &= a_{i,t,2,3}(a_{i,t,2,1}\omega_{i,t,x} - a_{i,t,1,1}\omega_{i,t,y}) \\ &\quad + a_{i,t,2,1}(a_{i,t,2,3}\omega_{i,t,x} - a_{i,t,1,3}\omega_{i,t,y}) \\ &\quad + a_{i,t,3,3}(a_{i,t,3,1}\omega_{i,t,x} - a_{i,t,1,1}\omega_{i,t,z}) \\ &\quad + a_{i,t,3,1}(a_{i,t,3,3}\omega_{i,t,x} - a_{i,t,1,3}\omega_{i,t,z}) \\ h_{i,t,1,8} &= a_{i,t,2,2}(a_{i,t,2,2}\omega_{i,t,x} - a_{i,t,1,2}\omega_{i,t,y}) \\ &\quad + a_{i,t,3,2}(a_{i,t,3,2}\omega_{i,t,x} - a_{i,t,1,2}\omega_{i,t,z}) \\ h_{i,t,1,9} &= a_{i,t,2,3}(a_{i,t,2,2}\omega_{i,t,x} - a_{i,t,1,2}\omega_{i,t,y}) \\ &\quad + a_{i,t,2,2}(a_{i,t,2,3}\omega_{i,t,x} - a_{i,t,1,3}\omega_{i,t,y}) \\ &\quad + a_{i,t,3,3}(a_{i,t,3,2}\omega_{i,t,x} - a_{i,t,1,2}\omega_{i,t,z}) \\ &\quad + a_{i,t,3,2}(a_{i,t,3,3}\omega_{i,t,x} - a_{i,t,1,3}\omega_{i,t,z}) \\ h_{i,t,1,10} &= a_{i,t,2,3}(a_{i,t,2,3}\omega_{i,t,x} - a_{i,t,1,3}\omega_{i,t,y}) \\ &\quad + a_{i,t,3,3}(a_{i,t,3,3}\omega_{i,t,x} - a_{i,t,1,3}\omega_{i,t,z}) \\ h_{i,t,2,1} &= -r_{i,t,x}v_{i,t,z} + r_{i,t,z}v_{i,t,x} \\ h_{i,t,2,2} &= a_{i,t,3,1}v_{i,t,x} - a_{i,t,1,1}v_{i,t,z} \\ &\quad - r_{i,t,x}(a_{i,t,2,1}\omega_{i,t,x} - a_{i,t,1,1}\omega_{i,t,y}) \\ &\quad + r_{i,t,z}(a_{i,t,3,1}\omega_{i,t,y} - a_{i,t,2,1}\omega_{i,t,z}) \\ h_{i,t,2,3} &= a_{i,t,3,2}v_{i,t,x} - a_{i,t,1,2}v_{i,t,z} \\ &\quad - r_{i,t,x}(a_{i,t,2,2}\omega_{i,t,x} - a_{i,t,1,2}\omega_{i,t,y}) \\ &\quad + r_{i,t,z}(a_{i,t,3,2}\omega_{i,t,y} - a_{i,t,2,2}\omega_{i,t,z}) \\ h_{i,t,2,4} &= a_{i,t,3,3}v_{i,t,x} - a_{i,t,1,3}v_{i,t,z} \\ &\quad - r_{i,t,x}(a_{i,t,2,3}\omega_{i,t,x} - a_{i,t,1,3}\omega_{i,t,y}) \\ &\quad + r_{i,t,z}(a_{i,t,3,3}\omega_{i,t,y} - a_{i,t,2,3}\omega_{i,t,z}) \\ h_{i,t,2,5} &= a_{i,t,3,1}(a_{i,t,3,1}\omega_{i,t,y} - a_{i,t,2,1}\omega_{i,t,z}) \\ &\quad - a_{i,t,1,1}(a_{i,t,2,1}\omega_{i,t,x} - a_{i,t,1,1}\omega_{i,t,y}) \\ h_{i,t,2,6} &= a_{i,t,3,2}(a_{i,t,3,1}\omega_{i,t,y} - a_{i,t,2,1}\omega_{i,t,z}) \end{aligned}$$

$$\begin{aligned} &\quad - a_{i,t,1,1}(a_{i,t,2,2}\omega_{i,t,x} - a_{i,t,1,2}\omega_{i,t,y}) \\ &\quad - a_{i,t,1,2}(a_{i,t,2,1}\omega_{i,t,x} - a_{i,t,1,1}\omega_{i,t,y}) \\ &\quad + a_{i,t,3,1}(a_{i,t,3,2}\omega_{i,t,y} - a_{i,t,2,2}\omega_{i,t,z}) \\ h_{i,t,2,7} &= a_{i,t,3,3}(a_{i,t,3,1}\omega_{i,t,y} - a_{i,t,2,1}\omega_{i,t,z}) \\ &\quad - a_{i,t,1,1}(a_{i,t,2,3}\omega_{i,t,x} - a_{i,t,1,3}\omega_{i,t,y}) \\ &\quad - a_{i,t,1,3}(a_{i,t,2,1}\omega_{i,t,x} - a_{i,t,1,1}\omega_{i,t,y}) \\ &\quad + a_{i,t,3,1}(a_{i,t,3,3}\omega_{i,t,y} - a_{i,t,2,3}\omega_{i,t,z}) \\ h_{i,t,2,8} &= a_{i,t,3,2}(a_{i,t,3,2}\omega_{i,t,y} - a_{i,t,2,2}\omega_{i,t,z}) \\ &\quad - a_{i,t,1,2}(a_{i,t,2,2}\omega_{i,t,x} - a_{i,t,1,2}\omega_{i,t,y}) \\ h_{i,t,2,9} &= a_{i,t,3,3}(a_{i,t,3,2}\omega_{i,t,y} - a_{i,t,2,2}\omega_{i,t,z}) \\ &\quad - a_{i,t,1,2}(a_{i,t,2,3}\omega_{i,t,x} - a_{i,t,1,3}\omega_{i,t,y}) \\ &\quad - a_{i,t,1,3}(a_{i,t,2,2}\omega_{i,t,x} - a_{i,t,1,2}\omega_{i,t,y}) \\ &\quad + a_{i,t,3,2}(a_{i,t,3,3}\omega_{i,t,y} - a_{i,t,2,3}\omega_{i,t,z}) \\ h_{i,t,2,10} &= a_{i,t,3,3}(a_{i,t,3,3}\omega_{i,t,y} - a_{i,t,2,3}\omega_{i,t,z}) \\ &\quad - a_{i,t,1,3}(a_{i,t,2,3}\omega_{i,t,x} - a_{i,t,1,3}\omega_{i,t,y}) \\ h_{i,t,3,1} &= r_{i,t,x}v_{i,t,y} - r_{i,t,y}v_{i,t,x} \\ h_{i,t,3,2} &= a_{i,t,1,1}v_{i,t,y} - a_{i,t,2,1}v_{i,t,x} \\ &\quad - r_{i,t,x}(a_{i,t,3,1}\omega_{i,t,x} - a_{i,t,1,1}\omega_{i,t,z}) \\ &\quad - r_{i,t,y}(a_{i,t,3,1}\omega_{i,t,y} - a_{i,t,2,1}\omega_{i,t,z}) \\ h_{i,t,3,3} &= a_{i,t,1,2}v_{i,t,y} - a_{i,t,2,2}v_{i,t,x} \\ &\quad - r_{i,t,x}(a_{i,t,3,2}\omega_{i,t,x} - a_{i,t,1,2}\omega_{i,t,z}) \\ &\quad - r_{i,t,y}(a_{i,t,3,2}\omega_{i,t,y} - a_{i,t,2,2}\omega_{i,t,z}) \\ h_{i,t,3,4} &= a_{i,t,1,3}v_{i,t,y} - a_{i,t,2,3}v_{i,t,x} \\ &\quad - r_{i,t,x}(a_{i,t,3,3}\omega_{i,t,x} - a_{i,t,1,3}\omega_{i,t,z}) \\ &\quad - r_{i,t,y}(a_{i,t,3,3}\omega_{i,t,y} - a_{i,t,2,3}\omega_{i,t,z}) \\ h_{i,t,3,5} &= -a_{i,t,1,1}(a_{i,t,3,1}\omega_{i,t,x} - a_{i,t,1,1}\omega_{i,t,z}) \\ &\quad - a_{i,t,2,1}(a_{i,t,3,1}\omega_{i,t,y} - a_{i,t,2,1}\omega_{i,t,z}) \\ h_{i,t,3,6} &= -a_{i,t,1,2}(a_{i,t,3,1}\omega_{i,t,x} - a_{i,t,1,1}\omega_{i,t,z}) \\ &\quad - a_{i,t,1,1}(a_{i,t,3,2}\omega_{i,t,x} - a_{i,t,1,2}\omega_{i,t,z}) \\ &\quad - a_{i,t,2,2}(a_{i,t,3,1}\omega_{i,t,y} - a_{i,t,2,1}\omega_{i,t,z}) \\ &\quad - a_{i,t,2,1}(a_{i,t,3,2}\omega_{i,t,y} - a_{i,t,2,2}\omega_{i,t,z}) \\ h_{i,t,3,7} &= -a_{i,t,1,3}(a_{i,t,3,1}\omega_{i,t,x} - a_{i,t,1,1}\omega_{i,t,z}) \\ &\quad - a_{i,t,1,1}(a_{i,t,3,3}\omega_{i,t,x} - a_{i,t,1,3}\omega_{i,t,z}) \\ &\quad - a_{i,t,2,3}(a_{i,t,3,1}\omega_{i,t,y} - a_{i,t,2,1}\omega_{i,t,z}) \\ &\quad - a_{i,t,2,1}(a_{i,t,3,3}\omega_{i,t,y} - a_{i,t,2,3}\omega_{i,t,z}) \\ h_{i,t,3,8} &= -a_{i,t,1,2}(a_{i,t,3,2}\omega_{i,t,x} - a_{i,t,1,2}\omega_{i,t,z}) \\ &\quad - a_{i,t,2,2}(a_{i,t,3,2}\omega_{i,t,y} - a_{i,t,2,2}\omega_{i,t,z}) \\ h_{i,t,3,9} &= -a_{i,t,1,3}(a_{i,t,3,2}\omega_{i,t,x} - a_{i,t,1,2}\omega_{i,t,z}) \\ &\quad - a_{i,t,1,2}(a_{i,t,3,3}\omega_{i,t,x} - a_{i,t,1,3}\omega_{i,t,z}) \\ &\quad - a_{i,t,2,3}(a_{i,t,3,2}\omega_{i,t,y} - a_{i,t,2,2}\omega_{i,t,z}) \\ &\quad - a_{i,t,2,2}(a_{i,t,3,3}\omega_{i,t,y} - a_{i,t,2,3}\omega_{i,t,z}) \\ h_{i,t,3,10} &= -a_{i,t,1,3}(a_{i,t,3,3}\omega_{i,t,x} - a_{i,t,1,3}\omega_{i,t,z}) \\ &\quad - a_{i,t,2,3}(a_{i,t,3,3}\omega_{i,t,y} - a_{i,t,2,3}\omega_{i,t,z}) \end{aligned}$$

$$\begin{aligned}
& + r_{i,t,y}(a_{i,t,2,3}\beta_{i,t,z} - a_{i,t,3,3}\beta_{i,t,y}) \\
& + \omega_{i,t,y}(a_{i,t,1,3}\omega_{i,t,y} - a_{i,t,2,3}\omega_{i,t,x}) \\
& + \omega_{i,t,z}(a_{i,t,1,3}\omega_{i,t,z} - a_{i,t,3,3}\omega_{i,t,x}) \\
s_{i,t,3,5} = & a_{i,t,1,1}(a_{i,t,1,1}\beta_{i,t,z} - a_{i,t,3,1}\beta_{i,t,x}) \\
& + \omega_{i,t,x}(a_{i,t,1,1}\omega_{i,t,y} - a_{i,t,2,1}\omega_{i,t,x}) \\
& - \omega_{i,t,z}(a_{i,t,2,1}\omega_{i,t,z} - a_{i,t,3,1}\omega_{i,t,y}) \\
& + a_{i,t,2,1}(a_{i,t,2,1}\beta_{i,t,z} - a_{i,t,3,1}\beta_{i,t,y}) \\
& + \omega_{i,t,y}(a_{i,t,1,1}\omega_{i,t,y} - a_{i,t,2,1}\omega_{i,t,x}) \\
& + \omega_{i,t,z}(a_{i,t,1,1}\omega_{i,t,z} - a_{i,t,3,1}\omega_{i,t,x}) \\
s_{i,t,3,6} = & a_{i,t,1,2}(a_{i,t,1,1}\beta_{i,t,z} - a_{i,t,3,1}\beta_{i,t,x}) \\
& + \omega_{i,t,x}(a_{i,t,1,1}\omega_{i,t,y} - a_{i,t,2,1}\omega_{i,t,x}) \\
& - \omega_{i,t,z}(a_{i,t,2,1}\omega_{i,t,z} - a_{i,t,3,1}\omega_{i,t,y}) \\
& + a_{i,t,1,1}(a_{i,t,1,2}\beta_{i,t,z} - a_{i,t,3,2}\beta_{i,t,x}) \\
& + \omega_{i,t,x}(a_{i,t,1,2}\omega_{i,t,y} - a_{i,t,2,2}\omega_{i,t,x}) \\
& - \omega_{i,t,z}(a_{i,t,2,2}\omega_{i,t,z} - a_{i,t,3,2}\omega_{i,t,y}) \\
& + a_{i,t,2,2}(a_{i,t,2,1}\beta_{i,t,z} - a_{i,t,3,1}\beta_{i,t,y}) \\
& + \omega_{i,t,y}(a_{i,t,1,1}\omega_{i,t,y} - a_{i,t,2,1}\omega_{i,t,x}) \\
& + \omega_{i,t,z}(a_{i,t,1,1}\omega_{i,t,z} - a_{i,t,3,1}\omega_{i,t,x}) \\
& + a_{i,t,2,1}(a_{i,t,2,2}\beta_{i,t,z} - a_{i,t,3,2}\beta_{i,t,y}) \\
& + \omega_{i,t,y}(a_{i,t,1,2}\omega_{i,t,y} - a_{i,t,2,2}\omega_{i,t,x}) \\
& + \omega_{i,t,z}(a_{i,t,1,2}\omega_{i,t,z} - a_{i,t,3,2}\omega_{i,t,x}) \\
s_{i,t,3,7} = & a_{i,t,1,3}(a_{i,t,1,1}\beta_{i,t,z} - a_{i,t,3,1}\beta_{i,t,x}) \\
& + \omega_{i,t,x}(a_{i,t,1,1}\omega_{i,t,y} - a_{i,t,2,1}\omega_{i,t,x}) \\
& - \omega_{i,t,z}(a_{i,t,2,1}\omega_{i,t,z} - a_{i,t,3,1}\omega_{i,t,y}) \\
& + a_{i,t,1,1}(a_{i,t,1,3}\beta_{i,t,z} - a_{i,t,3,3}\beta_{i,t,x}) \\
& + \omega_{i,t,x}(a_{i,t,1,3}\omega_{i,t,y} - a_{i,t,2,3}\omega_{i,t,x}) \\
& - \omega_{i,t,z}(a_{i,t,2,3}\omega_{i,t,z} - a_{i,t,3,3}\omega_{i,t,y}) \\
& + a_{i,t,2,3}(a_{i,t,2,1}\beta_{i,t,z} - a_{i,t,3,1}\beta_{i,t,y}) \\
& + \omega_{i,t,y}(a_{i,t,1,1}\omega_{i,t,y} - a_{i,t,2,1}\omega_{i,t,x}) \\
& + \omega_{i,t,z}(a_{i,t,1,1}\omega_{i,t,z} - a_{i,t,3,1}\omega_{i,t,x}) \\
& + a_{i,t,2,1}(a_{i,t,2,3}\beta_{i,t,z} - a_{i,t,3,3}\beta_{i,t,y}) \\
& + \omega_{i,t,y}(a_{i,t,1,3}\omega_{i,t,y} - a_{i,t,2,3}\omega_{i,t,x}) \\
& + \omega_{i,t,z}(a_{i,t,1,3}\omega_{i,t,z} - a_{i,t,3,3}\omega_{i,t,x}) \\
s_{i,t,3,8} = & a_{i,t,1,2}(a_{i,t,1,2}\beta_{i,t,z} - a_{i,t,3,2}\beta_{i,t,x}) \\
& + \omega_{i,t,x}(a_{i,t,1,2}\omega_{i,t,y} - a_{i,t,2,2}\omega_{i,t,x}) \\
& - \omega_{i,t,z}(a_{i,t,2,2}\omega_{i,t,z} - a_{i,t,3,2}\omega_{i,t,y}) \\
& + a_{i,t,2,2}(a_{i,t,2,2}\beta_{i,t,z} - a_{i,t,3,2}\beta_{i,t,y}) \\
& + \omega_{i,t,y}(a_{i,t,1,2}\omega_{i,t,y} - a_{i,t,2,2}\omega_{i,t,x}) \\
& + \omega_{i,t,z}(a_{i,t,1,2}\omega_{i,t,z} - a_{i,t,3,2}\omega_{i,t,x}) \\
s_{i,t,3,9} = & a_{i,t,1,3}(a_{i,t,1,2}\beta_{i,t,z} - a_{i,t,3,2}\beta_{i,t,x}) \\
& + \omega_{i,t,x}(a_{i,t,1,2}\omega_{i,t,y} - a_{i,t,2,2}\omega_{i,t,x}) \\
& - \omega_{i,t,z}(a_{i,t,2,2}\omega_{i,t,z} - a_{i,t,3,2}\omega_{i,t,y}) \\
& + a_{i,t,1,2}(a_{i,t,1,3}\beta_{i,t,z} - a_{i,t,3,3}\beta_{i,t,x}) \\
& + \omega_{i,t,x}(a_{i,t,1,3}\omega_{i,t,y} - a_{i,t,2,3}\omega_{i,t,x}) \\
& - \omega_{i,t,z}(a_{i,t,2,3}\omega_{i,t,z} - a_{i,t,3,3}\omega_{i,t,y}) \\
& + a_{i,t,2,3}(a_{i,t,2,2}\beta_{i,t,z} - a_{i,t,3,2}\beta_{i,t,y}) \\
& + \omega_{i,t,y}(a_{i,t,1,2}\omega_{i,t,y} - a_{i,t,2,2}\omega_{i,t,x}) \\
& + \omega_{i,t,z}(a_{i,t,1,2}\omega_{i,t,z} - a_{i,t,3,2}\omega_{i,t,x}) \\
s_{i,t,3,10} = & a_{i,t,1,3}(a_{i,t,1,3}\beta_{i,t,z} - a_{i,t,3,3}\beta_{i,t,x}) \\
& + \omega_{i,t,x}(a_{i,t,1,3}\omega_{i,t,y} - a_{i,t,2,3}\omega_{i,t,x}) \\
& - \omega_{i,t,z}(a_{i,t,2,3}\omega_{i,t,z} - a_{i,t,3,3}\omega_{i,t,y}) \\
& + a_{i,t,2,3}(a_{i,t,2,3}\beta_{i,t,z} - a_{i,t,3,3}\beta_{i,t,y}) \\
& + \omega_{i,t,y}(a_{i,t,1,3}\omega_{i,t,y} - a_{i,t,2,3}\omega_{i,t,x}) \\
& + \omega_{i,t,z}(a_{i,t,1,3}\omega_{i,t,z} - a_{i,t,3,3}\omega_{i,t,x}) \quad (50)
\end{aligned}$$

REFERENCES

- [1] Orbital Debris Quarterly News. (Feb. 2018). *The NASA Orbital Debris Program Office*. [Online]. Available: <https://www.orbitaldebris.jsc.nasa.gov/quarterly-news/pdfs/odqnv22i1.pdf>
- [2] Orbital Debris Quarterly News. (May 2018). *The NASA Orbital Debris Program Office*. [Online]. Available: <https://www.orbitaldebris.jsc.nasa.gov/quarterly-news/pdfs/odqnv22i2.pdf>
- [3] J.-C. Liou, "Active debris removal—A grand engineering challenge for the twenty-first century," in *Proc. AAS Spaceflight Mech. Meeting*, 2011, pp. 1–6.
- [4] M. Shan, J. Guo, and E. Gill, "Review and comparison of active space debris capturing and removal methods," *Prog. Aerosp. Sci.*, vol. 80, pp. 18–32, Jan. 2016.
- [5] J. L. Forshaw, G. S. Aglietti, N. Navarathinam, H. Kadhem, T. Salmon, A. Pisseloup, E. Joffre, T. Chabot, I. Retat, R. Axthelm, S. Barraclough, A. Ratcliffe, C. Bernal, F. Chaumette, A. Pollini, and W. H. Steyn, "RemoveDEBRIS: An in-orbit active debris removal demonstration mission," *Acta Astronautica*, vol. 127, pp. 448–463, Oct. 2016.
- [6] A. Flores-Abad, O. Ma, K. Pham, and S. Ulrich, "A review of space robotics technologies for on-orbit servicing," *Prog. Aerosp. Sci.*, vol. 68, pp. 1–26, Jul. 2014.
- [7] M. Oda, K. Kibe, and F. Yamagata, "ETS-VII, space robot in-orbit experiment satellite," in *Proc. IEEE Int. Conf. Robot. Autom.*, vol. 1, Apr. 1996, pp. 739–744.
- [8] R. B. Friend, "Orbital express program summary and mission overview," *Int. Soc. Opt. Photon. Sensors Syst. Space Appl. II*, vol. 6958, Apr. 2008, Art. no. 695803.
- [9] Z. Chu, Y. Ma, Y. Hou, and F. Wang, "Inertial parameter identification using contact force information for an unknown object captured by a space manipulator," *Acta Astronautica*, vol. 131, pp. 69–82, Feb. 2017.
- [10] Y. Murotsu, K. Senda, M. Ozaki, and S. Tsujio, "Parameter identification of unknown object handled by free-flying space robot," *J. Guid., Control, Dyn.*, vol. 17, no. 3, pp. 488–494, May 1994.
- [11] T. C. Nguyen-Huynh and I. Sharf, "Adaptive reactionless motion and parameter identification in postcapture of space debris," *J. Guid., Control, Dyn.*, vol. 36, no. 2, pp. 404–414, Mar. 2013.
- [12] T. Zhang, X. Yue, X. Ning, and J. Yuan, "Stabilization and parameter identification of tumbling space debris with bounded torque in postcapture," *Acta Astronautica*, vol. 123, pp. 301–309, Jun. 2016.
- [13] T. Zhang, X. Yue, B. Dou, and J. Yuan, "Online one-step parameter identification method for a space robot with initial momentum in postcapture," *J. Aerosp. Eng.*, vol. 33, no. 4, pp. 1–10, 2020.
- [14] O. Ma, H. Dang, and K. Pham, "On-orbit identification of inertia properties of spacecraft using robotics technology," in *Proc. AIAA Guid., Navigat. Control Conf. Exhib.*, 2007, p. 6815.
- [15] O. Ma, H. Dang, and K. Pham, "On-orbit identification of inertia properties of spacecraft using a robotic arm," *J. Guid., Control, Dyn.*, vol. 31, no. 6, pp. 1761–1771, Nov. 2008.
- [16] G. Feng, W. Li, H. Zhang, X. Xiao, J. Zhang, W. Li, and H. Zhang, "Probability distribution evolution algorithm to inertial parameters identification for space target," in *Proc. 4th Int. Conf. Syst. Informat.*, Nov. 2017, pp. 55–60.

- [17] S. Y. Nabavi Chashmi and S. M.-B. Malaek, "Fast estimation of space-robots inertia parameters: A modular mathematical formulation," *Acta Astronautica*, vol. 127, pp. 283–295, Oct. 2016.
- [18] K. Ayusawa, G. Venture, and Y. Nakamura, "Identifiability and identification of inertial parameters using the underactuated base-link dynamics for legged multibody systems," *Int. J. Robot. Res.*, vol. 33, no. 3, pp. 446–468, Mar. 2014.
- [19] W. Xu, Z. Hu, Y. Zhang, Z. Wang, and X. Wu, "A practical and effective method for identifying the complete inertia parameters of space robots," in *Proc. IEEE/RSJ Int. Conf. Intell. Robots Syst. (IROS)*, Sep. 2015, pp. 5435–5440.
- [20] W. Xu, Z. Hu, Y. Zhang, and B. Liang, "On-orbit identifying the inertia parameters of space robotic systems using simple equivalent dynamics," *Acta Astronautica*, vol. 132, pp. 131–142, Mar. 2017.
- [21] R. Featherstone, *Rigid Body Dynamics Algorithms*. New York, NY, USA: Springer, 2014.
- [22] R. Lampariello and G. Hirzinger, "Modeling and experimental design for the on-orbit inertial parameter identification of free-flying space robots," in *Proc. ASME Int. Design Eng. Tech. Conf. Comput. Inf. Eng. Conf.*, 2005, pp. 881–890.
- [23] R. Lampariello and G. Hirzinger, "Free-flying robots-inertial parameters identification and control strategies," in *Proc. ESA Workshop Adv. Space Technol. Robot. Autom.*, 2000, pp. 1–8.
- [24] C. P. Vyasrayani, T. Uchida, A. Carvalho, and J. McPhee, "Parameter identification in dynamic systems using the homotopy optimization approach," *Multibody Syst. Dyn.*, vol. 26, no. 4, pp. 411–424, Dec. 2011.
- [25] C. D. Sousa and R. Cortesão, "Physical feasibility of robot base inertial parameter identification: A linear matrix inequality approach," *Int. J. Robot. Res.*, vol. 33, no. 6, pp. 931–944, May 2014.
- [26] T. Lauß, S. Oberpeilsteiner, W. Steiner, and K. Nachbagauer, "The discrete adjoint method for parameter identification in multibody system dynamics," *Multibody Syst. Dyn.*, vol. 42, no. 4, pp. 397–410, 2018.
- [27] J. Wittenburg, *Dynamics of Multibody Systems*. New York, NY, USA: Springer, 2007.
- [28] F. Hamano, "Derivative of rotation matrix direct matrix derivation of well-known formula," in *Proc. Green Energy Syst. Conf.*, 2013, pp. 1–3.
- [29] X. R. Li and Y. Zhu, "Recursive least squares with linear constraints," *Commun. Inf. Syst.*, vol. 7, no. 3, pp. 287–312, 2007.



TENG ZHANG received the B.Eng. degree in flight vehicle design and engineering and the Ph.D. degree in flight vehicle design from the School of Astronautics, Northwestern Polytechnical University (NWPU), China, in 2009 and Spring 2020, respectively. His research interests include space robots, soft robots, gecko-like adhesives, numerical integration methods, and their applications.



XIAOKUI YUE (Member, IEEE) received the Ph.D. degree in flight vehicle design from the School of Astronautics, NWPU. He is currently a Professor and the Dean of the School of Astronautics, NWPU. His research interests include dynamics and control, space maneuver and operation, and relative navigation.



JIANPING YUAN received the Ph.D. degree in flight vehicle design from NWPU. He is currently a Professor with the School of Astronautics, NWPU. His research interests include dynamics and control, and space maneuver, and operation.

• • •